Tracing incorporation of heavy water into proteins for species-specific metabolic activity in complex communities

Robert Starke (robert.starke@biomed.cas.cz),[1,2] Kaitlyn Oliphant (koliphan@uoguelph.ca),[3] Nico Jehmlich (nico.jehmlich@ufz.de),[1] Stephanie Serena Schäpe (stephanie.schaepe@ufz.de),[1] Timo Sachsenberg (sachsenberg@gmail.com),[4,5] Oliver Kohlbacher (oliver.kohlbacher@uni-tuebingen.de),[4,5,6,7] Emma Allen-Vercoe (eav@uoguelph.ca),[3] and Martin von Bergen (martin.vonbergen@ufz.de)[1,8]

[1]Department of Molecular Systems Biology, Helmholtz-Centre for Environmental Research - UFZ, Leipzig, Germany

[2]Laboratory of Environmental Microbiology, Institute of Microbiology of the Czech Academy of Sciences, Prague, Czech Republic

[3]Department of Molecular and Cellular Biology, University of Guelph, Guelph, ON, Canada

[4]Applied Bioinformatics, Dept. of Computer Science, University of Tübingen, Tübingen, Germany

[5]Center for Bioinformatics, University of Tübingen, Germany

[6]Biomolecular Interactions, Max Planck Institute for Developmental Biology, Tübingen, Germany

[7]Institute for Translational Bioinformatics, University Hospital Tübingen, Tübingen, Germany

[8]Institute of Biochemistry, Faculty of Biosciences, Pharmacy and Psychology, University of Leipzig, Leipzig, Germany

Abstract

Stable isotope probing (SIP) approaches are a suitable tool to identify active organisms in bacterial communities, but adding isotopically labeled substrate can alter both the structure and the functionality of the community. Here, we validated and demonstrated a substrate-independent protein-SIP protocol using isotopically labeled water that captures the entire microbial activity of a community. We found that ^{18}O yielded a higher incorporation rate into peptides and thus comprised a higher sensitivity. We then applied the method to an *in vitro* model of a human distal gut microbial ecosystem grown in two medium formulations, to evaluate changes in microbial activity between a high-fiber and high-protein diet. We showed that only little changes are seen in the community structure but the functionality varied between the diets. In conclusion, our approach can detect species-specific metabolic activity in complex bacterial communities and more specifically to quantify the amount of amino acid synthesis. Heavy water makes possible to analyze the activity of bacterial communities for which adding an isotopically labeled energy and nutrient sources is not easily feasible.

Introduction

Culture-independent omic techniques are deployed to gain deeper insights into the structure and function of microbial communities [1]. Among these techniques, metaproteomics has gained popularity as a central tool in microbial ecology to decipher functional relationships between community members [2,3]. The relative metabolic activity of distinct community members can be assessed by stable isotope probing (SIP) approaches [4]. The two possibilities for labeling proteins are (a) the utilization of an energy or nutrient source with a heavy isotope or (b) the SILAC protocol, where labeled amino acids are added to the medium [5]. The latter method is problematic for microbiome research as it is restricted by the need to use a defined culture medium. All amino acids must be replaced by the labeled amino acids since the studied microorganisms must be auxotrophic for the labeled amino acids in order to incorporate isotopes and to detect incorporation [6]. Interestingly, the SILAC protocol could be used for bacteria that are not strictly auxotrophic but opportunistically rely on externally added amino acids [7]. However, this has to be established for every species individually and is thus not suitable for complex microbial communities. Consequently, studies utilizing protein-SIP have favored the isotopic labeling of an energy or nutrient source such as ^{13}C [4,8–12] or ^{15}N [11,13,14]. Protein-SIP yields two types of information. First, the relative isotope abundance (RIA) defined by the incorporation of heavy isotopes, which relates to the amount of substrate utilization by a microorganism. Second, the labeling ratio (LR) defined by the ratio of labeled and unlabeled peptides, which is related to protein turnover and thus microbial growth [15]. Careful cross-evaluation of all members in a studied community, especially in time-course experiments, can provide information on both the mechanism of substrate use and the overall contribution of

activity by each taxon [10]. However, the general drawback of these SIP studies is that only the activities of the substrate-degrading microbes are assessed. Thus, the activity of the microbial community in its entirety cannot be determined, especially if the community comprises of many inactive members [16]. Another drawback is the necessity of adding an isotopically labeled substrate to the medium and thus bearing the risk of altering the community. A possible solution was presented by Justice and colleagues who used two different labels in parallel: one for the substrate specificity (^{15}N) and one for determining the baseline metabolic activity (D_2O). This strategy was used to elucidate the relative activity of the microbial constituents present in acid mine drainage biofilms under different conditions [14]. More recently, it was also shown that ^{18}O-labeled water can be tracked in both DNA [17–19] and RNA [20,21] of active key players in microbial communities. In a recent protein-SIP study, the labelling of bacteria from an aquifer by D_2O was used for detecting anabolic uptake of aquifer specific carbon sources [22]. However, the toxicity of highly-deuterated water has been described for eukaryotes as it hampered cell division during the formation of the mitotic spindle [23] with cellular death as result [24]. In the methylotrophic bacterium *Brevibacterium methylicum*, the addition of 25 atom% D_2O resulted in a decrease of lag-period, yield of wet biomass and phenylalanine production whereas its generation time was comparable to growth in naturally abundant D_2O [25]. Similarly, completely deuterated medium caused a very wide proteomic response over many cell functional categories in addition with a down-regulation of translational proteins by 5% and a reduction in growth rate in *Escherichia coli* [26].

In order to provide to evaluate the incorporation of heavy water the aims of this study thus were to (i) determine the most suitable type of heavy water (D_2O or $H_2{}^{18}O$) for protein-SIP

78 experiments in microbial communities, (ii) provide a software tool for researchers to complete
79 protein-SIP studies utilizing heavy water, and (iii) demonstrate how a protein-SIP approach can
80 contribute to the analysis of key species and key pathways in a complex microbial community.
81

Results

Validation of isotope detection and correlation to metabolic activity

The MetaProSip software [27] was extended to trace the incorporation of deuterium and ^{18}O from mass spectra of peptides. These show either a continuous increase in peaks of with a higher content of heavy isotopes for deuterium (**Figure 1a**) or an increase of the M+2 peak for ^{18}O (**Figure 1d**). Deuterium incorporation of D5-ring labeled Angiotensin-II at different labeling ratios is shown in Figure 1b. The median RIA of these measurements was 7.5%, each with small variation indicated by the lower and upper quartiles. Further, unlabeled Angiotensin-II was incubated in D_2O for 24 h, and measured by direct infusion to ensure minimal exposure to unlabeled water. The abiotic incorporation of deuterium greatly diminished after eight minutes (**Figure S1**). In order to control the accuracy of quantifying ^{18}O incorporation, BSA was tryptically digested in ^{18}O-labeled water at different concentrations. This digestion resulted in median RIA of 24.8%, 30.1%, and 51.5% when the peptides were incubated with 25%, 37.5%, and 50%, and of the ^{18}O label, respectively, each showing small variation indicated by the lower and upper quartiles (**Figure 1e**). The cultivation of *E. coli* K12 in 4 mL volumes of LB medium resulted in higher amounts of labeled peptides with $H_2{}^{18}O$ (**Figure 1f**) as compared to D_2O (**Figure 1c**), which increased in the exponential phase but decreased in the stationary phase. The RIA values were lower with D_2O but stagnated in the early exponential growth phase when 25% label was applied, whereas increasing RIA values were found with 50% label of both ^{18}O and D until the stationary phase.

Identification of activity in a defined human fecal microbial community

After establishing the correlation between metabolic activity and deuterium and ^{18}O incorporation in a pure culture, the impact of specific diets on a defined microbial community derived from a human fecal sample was to be determined. The defined community was chosen to provide a stable *in vitro* setup that could be useful for future microbiome research. Briefly, the microbial community was grown in a heavy fiber and a heavy protein diet in addition to 25% heavy water, either as D_2O or $H_2{}^{18}O$. A dosage of 25% isotopically labeled water was chosen by trial-and-error to yield sufficient incorporation into protein but avoid the reduction of activity of individual organisms. A difference in growth medium formulation, representing a high-fiber diet and a high-protein diet, was utilized to evaluate shifts in microbial activity. We chose to assess these diets because high-protein, low-carbohydrate interventions represent a popular weight-loss strategy and because we expected a strong effect on the synthesis of amino acids by this comparison. After an incubation time of 12h, the proteins were analyzed for label-free quantitation (metaproteomics) and incorporation of isotopes (protein-SIP), each in triplicates (**Figure 2a**). The experiments demonstrated high reproducibility between three biological replicates each that separated the RIA from deuterium and 18-oxygen. Specifically, incubation with deuterium resulted in median RIA values of 5.1% for high-protein and 5.3% for high-fiber diets (**Figure 2b**). Otherwise, ^{18}O resulted in high reproducibility and RIA values of 13.8% for high-protein and 14.8% for high-fiber diets (**Figure 2b**). Plotting the labelling ratio (LR) versus RIA for the 20 most active taxa (Supplementary information, **Table S1**) revealed different patterns for both labelling approaches. For 18-oxygen, no statistically significant correlation between LR and RIA was observed (R^2 =0.05, P =0.35). However, for deuterium, a positive and significant correlation was detected (R^2 =0.23, P =0.03) (**Figure 2c**). The RIA as a direct measure for the

synthesis of amino acids is of specific interest since the protein-rich diet provides a higher amount of externally available amino acids. Consequently, there are only a few taxa in the lower left quarter of the RIA plot for deuterium.

Identification of active key players in a defined human fecal microbial community

For additional functional information, we analyzed the relative abundances (RA) of taxa from the metaproteome and the protein-SIP approach together with the RIA of the most abundant species in the defined microbial community (**Figure 3**). These species comprised of at least 90% of the relative abundance in both the metaproteome and the protein-SIP approach. The metaproteome-based community structure showed similar abundances across diets and labels, and was dominated by *B. uniformis*, *B. thetaiotaomicron*, *B. ovatus*, *B. eggerthii*, *B. cellulosilyticus* and *A. muciniphila*. In the protein-SIP of both hydrogen and 18-oxygen labeled water, most labeled peptides (as relative abundance - RA) were assigned to *A. muciniphila*, followed by *B. vulgatus*, *B. ovatus*, *B. uniformis* and *B. thetaiotaomicron*. Differently, the commonly used relative isotope abundance (RIA) showed similar averages in the detected species. Lastly, we analyzed the differences between the relative functional contributions of the defined microbial community peptides between high fiber and high protein diets (**Figure 4**). In total, 236 proteins showed a significantly higher abundance on high fiber diet as compared to 298 proteins on high protein diet. Proteins were assigned to clusters of orthologous groups (COGs) and the relative abundance of unlabeled peptides in the metaproteome data was compared. The COG classes cell cycle control, cell division, chromosome partitioning (D, P =0.20), amino acid transport and metabolism (E, P =4.26E-11), cell wall/membrane/envelope biogenesis (M, P =0.25), inorganic ion transport and metabolism (P, P =0.06), general function prediction

only (R, P =0.88), intracellular trafficking, secretion, and vesicular transport (U, P =0.96) and defense mechanisms (V, P =0.84) were more abundant in the high fiber diet, whereas translation, ribosomal structure and biogenesis (J, P =4.65E-26), post-translational modification, protein turnover, and chaperones (O, P =1.95E-23) and function unknown (S, P =2.06E-5) were higher in the high protein diet. Of these, the classes amino acid transport and metabolism (E), translation, ribosomal structure and biogenesis (J), post-translational modification, protein turnover, and chaperones (O) and function unknown (S) were significantly changed (P <0.05) (for more information on individual proteins, see supporting information **Table S4**).

Pathway analysis of general and specific functionality

On high fiber diet, translated genes were significantly (P <0.05) enriched for the KEGG categories Metabolic pathways, Biosynthesis of secondary metabolites, Biosynthesis of amino acids, Microbial metabolism in diverse environments, Aminoacyl-tRNA biosynthesis, Purine metabolism, Arginine and proline metabolism, Carbon metabolism, Alanine; aspartate and glutamate metabolism, and Ribosome (for more information on pathway analysis, see supporting information **Table S5**). Otherwise, on high protein diet, the highest enrichment FDR was found for Ribosome. In addition to Metabolic pathways, Biosynthesis of secondary metabolites, Carbon metabolism, Microbial metabolism in diverse environments, Biosynthesis of amino acids, and Purine metabolism, significant enrichments (P <0.05) were observed for Glycolysis / Gluconeogenesis, Amino sugar and nucleotide sugar metabolism, and Fructose and mannose metabolism. On the level of ECOCYC, the three most significant pathway enrichments were superpathway of histidine; purine; and pyrimidine biosynthesis, purine nucleotides de novo biosynthesis I, and adenosine nucleotides de novo biosynthesis regardless the diet. On high fiber

diet, starch degradation V, arginine biosynthesis II (acetyl cycle), arginine biosynthesis I, 5-aminoimidazole ribonucleotide biosynthesis II, superpathway of 5-aminoimidazole ribonucleotide biosynthesis, purine nucleotides de novo biosynthesis II, and superpathway of pyrimidine ribonucleotides de novo biosynthesis were significantly enriched as opposed to glycolysis III (glucokinase), glycolysis I, GDP-mannose biosynthesis, gluconeogenesis I, superpathway of glycolysis; pyruvate dehydrogenase; TCA; and glyoxylate bypass, superpathway of glycolysis and Entner-Doudoroff, and TCA cycle VI (obligate autotrophs) on high protein diet.

Discussion

Detecting species-specific metabolic activity by stable isotope probing approaches without disturbing the community is a highly relevant objective in microbial ecology. As such, deuterated water has been used previously to evaluate the protein turnover in both mammals and microorganisms [14,28]. Here, we present a novel method for quantifying system-wide microbial activity through tracing of isotopically-labeled water in proteins, and we have demonstrated its use in an *in vitro* model of a human distal gut microbial ecosystem. The computational methods required to analyze heavy-labeled water were integrated into the freely available bioinformatics tool MetaProSIP [27].

Validation of isotope detection and correlation to metabolic activity

As MetaProSIP only contained the pipelines of ^{13}C and ^{15}N, we first validated each pipeline by experimentally comparing the amount of incorporated isotopes (RIA) to the theoretical values of peptide standards labeled with deuterium and ^{18}O, respectively. This was necessary as the retention time of deuterated peptides can change and must be accounted for by searching for the incorporation pattern not only at one time point as it was done for the other isotopes. In addition, the mass change of +2 of the heavy compared to the light isotope of oxygen required a different algorithm of determining RIA. For deuterium, the experimental RIA was slightly higher than the theoretical value for the purchased peptide Angiotensin-II in which five hydrogen atoms were replaced by deuterium; however, this deviation was within the expected 1% range of analytical inaccuracy and should thus be disregarded. For ^{18}O, commercially available BSA was tryptically digested in different concentrations of ^{18}O-labeled water, as an ^{18}O-labeled peptide was unavailable because of the isotope's interference with the fmoc peptide synthesis strategy

198 [29]. The applicability of introducing ^{18}O by proteolytic digestion has been described before [30].
199 Briefly, when a protein is tryptically digested, one oxygen molecule from water is introduced at
200 the C-terminus [31]. In our experiment, tryptic digestion in 50% and 25% $H_2{}^{18}O$ yielded peptides
201 with a median RIA of 50% and 25%, respectively, but 37.5% $H_2{}^{18}O$ resulted in a slightly lower
202 median RIA of 30%. The isotope distribution of the measured labeled peptides thus matched
203 expectation, and a lower isotope abundance with 37.5% $H_2{}^{18}O$ could be sensitive to large
204 deviations since only one oxygen is replaced during protein hydrolysis. In fact, peptides with
205 incorporation clustered at RIA values of 25% and 50% when 50% $H_2{}^{18}O$ was applied; clearly
206 indicating the stochastic effect. As this variability can be ascribed to the experimental rather than
207 technical factors of the pipeline, especially in the case of deuterium, we concluded that our
208 pipeline accurately quantified the RIA of both D and ^{18}O.
209 *The differentiation between generalists and specialists using the incorporation of heavy water*
210 After confirming the accuracy and precision of the pipeline, the method was applied to a
211 diverse but defined microbial community (63 strains) in an *in vitro* setting to demonstrate its
212 usefulness in microbiome research. A dosage of 25% isotopically labeled water was chosen as the
213 RIA was not significantly different between this dose and the highest dosage tested in *E. coli*,
214 suggesting that there was no substantial improvement in isotope incorporation after increasing
215 the amount to 50% for stationary growth. A difference in growth medium formulation,
216 representing a high-fiber diet and a high-protein diet, was utilized to evaluate shifts in microbial
217 activity. We chose to assess these diets because high-protein, low-carbohydrate interventions
218 represent a popular weight-loss strategy and because we expected a strong effect on the
219 synthesis of amino acids by this comparison. For the low-carbohydrate intervention, concerns

have been raised over the impact of such dietary strategies on colonic health, as the gut microbiota is known to convert complex polysaccharides into beneficial nutrients for intestinal epithelial cells (*e.g.,* short-chain fatty acids [32,33]), whereas proteolytic products include compounds which can behave as gut irritants, including nitrosamines and heterocyclic amines [33]. Examining if the lower carbohydrate availability impacted microbial functional activity was thus of interest. The experiments demonstrated high reproducibility between replicates, with small lower and upper quartiles for both RIA and RA. There was no significant difference in the RIA between diets; however, the values were roughly double the RIA of the *E. coli* experiments.

Additionally, the RIA for ^{18}O was nearly three times higher than the RIA for deuterium, in all cases (including the *E. coli* experiments). These observations can be attributed to the mechanism of deuterium incorporation into proteins [28]. Deuterium will readily equilibrate with normal water and be taken up by a bacterial cell, after which it is incorporated into non-essential amino acids during specific enzymatic steps in their biosynthetic pathways. These labeled amino acids can then be subsequently added to proteins. The method of ^{18}O incorporation is expected to be similar, but unlike deuterium, in which only C-H bonds are reliable due to abiotic H-D exchange of acidic hydrogens when proteins are in contact with unlabeled water [34] as during sample preparation, all incorporated ^{18}O atoms are likely to be retained. We observed a higher RIA for ^{18}O, consistent with this expectation. Admittedly, the H-D exchange of acidic hydrogens could be mitigated by not only performing the cultivation but also the sample preparation and the measurement in the similar atom% of D_2O, potentially resulting in higher RIA values that could be different on species level unlike the incorporation into C-H bonds or of ^{18}O. However, the LC-MS/MS measurement could be tricky as adding D_2O as solvent will not only change the

242 retention time of the peptides but also the ionization efficiency as H_2O and D_2O droplets may
243 evaporate differently. Logically, further tests are needed to fully understand the potential impact
244 of added D_2O to the measurement. As of now, the incorporation rates of D into C-H bonds are
245 similar as before [22] with similar patterns as ^{18}O and highly reproducible. The routes of
246 incorporation of ^{18}O vary for the different amino acids (Figure 5). The incorporation follows three
247 main roads: firstly through pyruvate into leucine/isoleucine, secondly through α-ketoglutarate
248 into glutamate, histidine, arginine, proline and thirdly through oxaloacetate into aspartate,
249 threonine, lysine, asparagine, and methionine. Nevertheless, the incorporation is at this point
250 mostly unstable since for stable incorporation the oxygen needs to be incorporated at a C-atom
251 other than the C-terminus since the oxygen would be lost during peptide-bond-formation.
252 Therefore only the oxygen incorporated into the side chain of glutamine and asparagine can be
253 considered stable also after peptide bond formation. Hence, actual incorporation will be lost by
254 both labelling with D_2O and $H_2{}^{18}O$ but the leftover labelling appears to be highly reproducible,
255 yielding similar active organisms and their specific activity. However, we found no definite
256 explanation as to why the relationship between RIA and LR regarding the two diets were opposite
257 in the 20 most active species but both RIA and LR were generally higher in the high protein diet
258 with both isotopes.

259 Microbial species of different taxa possess a diversity of auxotrophy for amino acids and
260 alter their requirements for *de novo* amino acid biosynthesis depending on the concentration of
261 these amino acids in the environment [35,36]. In our experiments, batch cultures of *E. coli* K12 in
262 protein-rich media would have had access to abundant amino acids by protein hydrolysis, such
263 that a relatively lower amount of *de novo* amino acid biosynthesis would be required (and thus a

lower RIA). In contrast, members of a complex microbial community such as our derived fecal ecosystem compete for available amino acids in a less protein-rich medium, necessitating a higher degree of *de novo* amino acid biosynthesis (and thus a higher RIA). Most healthy human fecal samples indeed possess a relatively low concentration of amino acids in the range of 0-20 μg/mL [37], and the maintenance of these levels is thought of as an innate immune defense; conditions that give rise to excess amino acids in this environment (*e.g.,* in the case of antibiotic treatment) can be exploited by opportunistic pathogens such as *Clostridioides difficile* [38].

We determined that the RIA was similar for most species within our defined microbial community, which we believe further validated our experimental approach. Amino acid biosynthetic pathways are generally highly conserved amongst the bacterial families present in the intestine [35], and although differences in amino acid auxotrophy have been reported [35,36], our analysis suggested that this phenomenon is not a common feature. Our findings are in agreement with those of Price *et al.* [36], who recently tested the growth of a range of genera in minimal media and found that almost all of them grew without supplementation, despite only half of them being predicted to be auxotrophic for certain amino acids. It was concluded that our current knowledge of amino acid biosynthetic pathways is insufficient, and indeed most free-living microorganisms may be capable of synthesizing all 21 proteinogenic amino acids.

The differentiation between generalists and specialists using the incorporation of heavy water

One strength to our approach, when applied to microbial ecosystems, is that it has the ability to distinguish microbial generalists from specialists, in a non-predictive manner. We found that the majority of the most active microbes did not experience a shift in the ranking of RA between diets. Generalists are able to shift their metabolism when substrates are changed

without sacrificing growth. An example of a generalist genus is *Bacteroides,* members of which possess a wide variety of polysaccharide and protein degradative capabilities. Six *Bacteroides* species were components of our defined microbial community, and these displayed the most activity in our experiment. Interestingly, even after the switch in diets, the four *Bacteroides* did not experience a rank change in RA amongst themselves. Previous work has indicated that *Bacteroides* species do not utilize polysaccharides in a random fashion, but rather have an inherent, strain-specific hierarchy of preference, which is retained in a community setting [39,40]. We suspect that if a strain of *Bacteroides* was presented with an abundance of a given preferred substrate, it would increase its activity relative to the other species present in the community. Our media formulations were similar with respect to the ratio of the majority of component fiber sources, and increasing protein content did not alter the activity ranking of the *Bacteroides* species, indicating that none of these species favoured protein degradation when carbohydrates were still available. This observation is in line with previous work that showed when there is an abundance of complex carbohydrates in the gut ecosystem environment, amino acids tend to be utilized anabolically [45]. Thus, our work adds compelling evidence to the premise that behavioral shifts of the gut microbiota in response to diet are primarily complex carbohydrate-driven [41–43].

In addition to *Bacteroides*, members of the *Firmicutes* and the *Actinobacteria* are capable of primary polysaccharide degradation in the gut. However, unlike *Bacteroides*, members of the *Firmicutes* and *Actinobacteria* tend to be specialists, possessing a limited repertoire of fibers they can utilize, with a tendency to favor starch-derived polymers [44,45]. Indeed, *R. bromii,* a known starch-degrading specialist that has been previously shown to have low RA within a healthy gut

ecosystem by 16S rRNA gene sequencing when starch is limiting [43,46], experienced a drop in RA by protein-SIP upon introduction of the high protein medium. Therefore, it was ultimately the specialist that exhibited an alteration of activity upon dietary change. In contrast, *A. muciniphila*, a mucin-degrading specialist [41], did not alter its relative activity between shifts in growth media. This observation could simply be attributed to the equal amount of mucin in both media (**Table S2**); however, *A. muciniphila* has been previously reported to increase in RA within irritable bowel syndrome and obese subjects' fecal microbial ecosystems by 16S rRNA sequencing after fiber [47] or oligofructose supplementation [48]. This is counterintuitive, given that *A. muciniphila* is not known to be able to utilize inulin as a sole carbon source [49]. It is possible that *A. muciniphila* indirectly benefits from fiber intake, by partaking in cross-feeding and/or expanding after a decrease in competition. In our experiment, there was enough dietary substrate to prevent a notable difference in such proposed mechanisms, but future work utilizing our technique could evaluate if withholding complex carbohydrates indeed diminish the activity of *A. muciniphila*.

Similar to our findings, multiple studies have also reported only minor alterations in microbial community composition after dietary change [32,43,50], and the stability of the gut microbiota over time is purportedly robust, with 60% retention of strains after five years [50]. Generalist *Bacteroides* in particular are known to have a higher retention rate than more specialist species [51]. When more dramatic changes have been observed, this was usually associated with more extreme dietary intervention [51] or with the maintenance of specific dietary patterns over the long-term [50]. Further, the context in which a particular dietary substrate is taken also appears to be important, as one study demonstrated that the common

prebiotic, inulin, only sufficiently prevented microbial conversion of dietary nitrogen when digested with the test diet and not several hours afterwards [52]. Our future goals include tracing isotopically labeled water in an *in vitro* model to evaluate the differential carbohydrate ratios that drive gut microbiota metabolism.

Differences in microbiome functionality between the two medium formulations

Lastly, despite only minor changes in microbial community composition derived from unlabeled and isotopically labeled peptides, we found significant differences in the relative abundance of unlabeled peptides between the diets when clustered into functional groups (COGs). Consistent with our hypothesis of *de novo* amino acid biosynthesis, we found proteins involved with amino acid transport and metabolism to be higher on high fiber (the diet with less protein content) as compared to proteins involved in translation, ribosomal structure and biogenesis (J) and post-translational modification, protein turnover, and chaperones (O) that were elevated on high protein. Logically, if a higher amount of proteins is available is the medium, the organisms will invest less energy into the synthesis of amino acids but rather digest and/or modify the proteins from the medium. In compliance, pathway analysis revealed that the translated genes on the high protein diet were directly affiliated with translation and energy such as TCA cycle, glycolysis and gluconeogenesis while, when grown on the high fiber diet, more resources must be spend towards amino acid and protein synthesis. We thus hypothesize that even when the community structure and its active key players did not change upon different dietary conditions, the functions may have. It is, however, questionable if a different phylogenomic database as annotation tool will yield comparable results given that the microbiome functionality is likely to be underestimated [53,54].

Concluding remarks

In summary, (i) we have validated two novel pipelines for evaluating microbial activity through tracing isotopically labeled heavy water and successfully applied them to a defined microbial community cultured *in vitro* in a model emulating the distal human gut. The methodology described here is applicable to a variety of both animal- and environment-associated microbiomes and *in vitro* models and (ii) was implemented into the freely available tool of MetaProSIP. Unlike other SIP-applications and applicable for both isotopes, the commonly used relative isotope abundance (RIA) yielded similar values among the active bacterial species whereas the relative abundance (RA) of labeled peptides separated the degree of activity among those. The relative functional contribution of microbiota constituents is a key question, in which the answer will further improve our understanding of these complex ecosystems, and (iii) we suggest that the use of relative abundance of labeled peptides in heavy water protein-SIP can help to address critical hypotheses in complex ecosystem dynamics. Notably, protein-SIP with heavy water was capable to differ between a stress response at permissive temperatures and a general growth activity at retardant temperatures in *E. coli* K12 despite both having a comparable RA of labeled peptides. However, the influence on growth by higher atom% of heavy water, especially of D_2O on eukaryotes, must be taken into consideration when systems with non-bacterial species are examined.

Materials and Methods

Validation of isotope detection

In order to validate the MetaProSIP v2.0 pipeline (see Supplementary information for more information), ring-D5 at phenylalanine labeled Angiotensin-II (Bachem, Bubendorf, Switzerland) was mixed with unlabeled Angiotensin-II (Bachem, Bubendorf, Switzerland) at different labeling ratios (20, 40, 60, 80 and 100%) in 0.1% formic acid, in triplicate. For ^{18}O incorporation analysis, bovine serum album (BSA) was tryptically digested in different concentrations of $H_2{}^{18}O$ (99 atom%, Sigma-Aldrich), as previously described [30].

The strain *E. coli* K12 obtained from the Leibniz-Institut DSMZ - Deutsche Sammlung von Mikroorganismen und Zellkulturen GmbH (DSM 498) was grown in 2 mL LB-Miller medium supplemented with 2 g L^{-1} glucose and 2 mL ddH_2O. For the protein-SIP experiments, the water was replaced by either 2 mL $H_2{}^{18}O$ (99 atom%, Sigma-Aldrich) or D_2O (99.9 atom%, Sigma-Aldrich). To begin the incubation, 50 µL of a pre-grown culture under similar conditions at an optical density of one was added. Cultures were incubated at 37°C and stopped after subsampled after two, four and six hours. For this, 1 mL was centrifuged at 13 200 rpm, 4°C for 10 min (Eppendorf Centrifuge 5430 R, Eppendorf North America, New York, USA). Cell pellets were resuspended in 1 mL Tris buffer (20 mM Tris/HCl pH 6.8, 0.1% SDS) and ultrasonicated for 10 min. After centrifugation as described above, the supernatant was subsequently collected and stored at -20°C.

Bioreactor operation and batch culture processing

Two Multifors bioreactors (Infors, Basel/Bottmingen, Switzerland) were operated as *in vitro* models of the distal human gut with working volumes of 500 mL as previously described

393 [55], but with custom medium formulations representing different diets [56] to accommodate a
394 single vessel system [57] (**Table S2**). Both bioreactors were inoculated with a defined microbial
395 community isolated from a healthy human fecal sample that was described before [55],
396 comprising of 63 bacterial strains from six phyla (**Table S3**). The microbial ecosystems were
397 allowed two weeks to equilibrate. Batch cultures were then set up using harvested bioreactor
398 material and the isotopically labeled water. Each batch culture comprised 2 mL of the harvested
399 bioreactor contents, 1 mL of the pre-reduced, double-strength respective medium used in the
400 bioreactor, and 1 mL of the isotopically labeled water, with ddH_2O used as a control. In total,
401 18 x 4 mL batch cultures were prepared, with triplicates per medium formulation water type. The
402 batch cultures were incubated in an anaerobic chamber (Baker Ruskinn, Sanford, ME, USA) at
403 37°C with a gas mixture of 5:5:90 H_2:CO_2:N_2 for 12 h, after which the culture contents were evenly
404 divided into two aliquots. A sample of the bioreactor contents for each medium formulation was
405 collected upon batch culture preparation.
406 Two aliquots of each sample were centrifuged as described above. For each sample, one
407 cell pellet was used for DNA and the other for protein extraction. DNA extraction was completed
408 via the QIAamp DNA Stool Mini Kit (Qiagen, Germantown, MD, USA) following the manufacturer's
409 directions with slight modifications: the cell pellet was resuspended in 200 µL of 100 mM Tris-
410 HCl, 10 mM EDTA, pH 8.0 buffer prior to the first step, the initial high-temperature incubation
411 was 95°C for 15 min, and the final elution of DNA was carried out using 50 µL of the elution buffer,
412 which was pre-warmed at 50°C. All DNA samples were stored at 4°C after processing. The protein
413 extraction was completed by first resuspending the cell pellet in 1 mL of 0.4% (w/v) sodium
414 dodecyl sulfate in 100 mM Tris-HCl, 5 mM EDTA, 0.5 mM NaCl, pH 8.0 buffer with 0.1 µL of

protease inhibitor cocktail set III (Calbiochem, Etobicoke, ON, Canada) added. The samples were then bead-beaten with 0.2 g of zirconia beads (Biospec Products Inc., Bartlesville, OK, USA) using the Digital Disruptor Genie (Scientific Industries Inc., New York City, NY, USA) at 3 000 rpm for 4 min, followed by incubation at 60°C for 15 min, before being sonicated using the Ultrasonic Processor XL2020 (Mandel Scientific, Guelph, ON, Canada) on ice for a total of 2 min with 10-s pulse, 10-s off intervals. Samples were subsequently centrifuged as described above, and the supernatant containing the protein extract was collected and stored at -20°C.

Sample preparation, mass spectrometry and isotope incorporation

The supernatants were incubated with fivefold volumes of 100 mM ammonium acetate in methanol overnight. After centrifugation as described above, cell pellets were resuspended in 1 mL ice-cold acetone and centrifuged again. The entire volume of the samples was used for one-dimensional (1D) gel electrophoresis without prior determination of the protein amount. Air-dried protein pellets were suspended in 30 µL 1x Laemmli buffer [58], dissolved via ultrasonication, and incubated with shaking at 500 rpm, 90°C for 10 min. Samples were centrifuged as described above to remove precipitates before loading on sodium dodecyl sulfate gels (4% stacking gel and 12% separating gel). Electrophoresis was performed at 10 mA per gel. Polypeptides were stained by colloidal Coomassie Brilliant Blue G-250 (Roth, Kassel, Germany). Gel lanes were cut into pieces for each sample, and in-gel tryptic digestion was performed as described before [59] (see Supplementary information for more information).

Tryptic peptides were analyzed by UPLC Q Exactive-MS/MS. The peptides were eluted using a linear gradient of 125 min with 4-55% solvent B (80% acetonitrile, 0.08% formic acid) or, in case of the validation, using a linear gradient of 60 min with 4-55% solvent B (80% acetonitrile,

0.08% formic acid). Continuous scanning of eluted peptide ions was carried out between 350 and 1 550 *m/z* at a resolution of 120 000 and a maximum injection time of 120 ms, automatically switching to MS/MS HCD mode using normalized collision energy of 30%. The obtained raw data was processed with database searches by Thermo Proteome Discoverer (v1.4.1.14; Thermo Fisher Scientific, Waltham, MA, USA). Searches were performed using the Sequest HT algorithm with the following parameters: tryptic cleavage with maximal two missed cleavages, a peptide tolerance threshold of ±10 ppm, an MS/MS tolerance threshold of ±0.02 Da, carbamidomethylation at cysteines as static modifications and oxidation of methionines as variable modifications. Searches were performed against the genome of *E. coli* K12 (Uniprot, 02/16/2016) or the combined metagenome consisting of the species present in the defined microbial community (**Table S3**). Only protein groups with at least one unique peptide and high confidence (false discovery rate (FDR) <0.01) were considered. The FDR was determined by a concatenated target-decoy database searches. The MetaProSIP tool [27] of OpenMS [60] was used to identify the incorporation of stable isotopes. Raw data files were converted to mzML files using MSConvert of ProteoWizard. The computational workflow then detected and identified signals of eluting peptides in the mass spectra using a stricter fragment mass tolerance of ±0.02 Da. This information formed the input to the MetaProSIP tool that calculates RIA and LR based on detected isotopic mass traces (*m/z* tolerance of ±10 ppm, intensity threshold of 1,000, and an isotopic trace correlation threshold of 0.7).

Pathway analysis

The fold change as log2 of the difference between the abundance of peptides on the high fiber and the high protein diet was estimated as average for all peptides of one protein. The associated genes that were enriched by at least 10% on either diet were analyzed for global (KEGG) and specific functionality (ECOCYC) using ShinyGO v0.61 (http://bioinformatics.sdstate.edu/go/) and the top 10 functional classes were obtained with enrichment FDR-

References

[1] F.A. Herbst, V. Lünsmann, H. Kjeldal, N. Jehmlich, A. Tholey, M. von Bergen, J.L. Nielsen, R.L. Hettich, J. Seifert, P.H. Nielsen, Enhancing metaproteomics-The value of models and defined environmental microbial systems, Proteomics. (2016). doi:10.1002/pmic.201500305.

[2] M. Von Bergen, N. Jehmlich, M. Taubert, C. Vogt, F. Bastida, F.A. Herbst, F. Schmidt, H.H. Richnow, J. Seifert, Insights from quantitative metaproteomics and protein-stable isotope probing into microbial ecology, ISME J. (2013). doi:10.1038/ismej.2013.78.

[3] F. Bastida, N. Jehmlich, K. Lima, B.E.L. Morris, H.H. Richnow, T. Hernández, M. von Bergen, C. García, The ecological and physiological responses of the microbial community from a semiarid soil to hydrocarbon contamination and its bioremediation using compost amendment, J. Proteomics. (2016). doi:10.1016/j.jprot.2015.07.023.

[4] N. Jehmlich, F. Schmidt, M. Von Bergen, H.H. Richnow, C. Vogt, Protein-based stable isotope probing (Protein-SIP) reveals active species within anoxic mixed cultures, ISME J. (2008). doi:10.1038/ismej.2008.64.

[5] X. Chen, S. Wei, Y. Ji, X. Guo, F. Yang, Quantitative proteomics using SILAC: Principles, applications, and developments, Proteomics. (2015). doi:10.1002/pmic.201500108.

[6] J. V. Quijada, N.D. Schmitt, J.P. Salisbury, J.R. Auclair, J.N. Agar, Heavy sugar and heavy water create tunable intact protein mass increases for quantitative mass spectrometry in any feed and organism, Anal. Chem. (2016). doi:10.1021/acs.analchem.6b03234.

[7] S.A. Müller, S.R. Pernitzsch, S.B. Haange, P. Uetz, M. von Bergen, C.M. Sharma, S. Kalkhof, Stable isotope labeling by amino acids in cell culture based proteomics reveals differences in protein abundances between spiral and coccoid forms of the gastric pathogen Helicobacter pylori, J. Proteomics. (2015). doi:10.1016/j.jprot.2015.05.011.

[8] F.A. Herbst, A. Bahr, M. Duarte, D.H. Pieper, H.H. Richnow, M. von Bergen, J. Seifert, P. Bombach, Elucidation of in situ polycyclic aromatic hydrocarbon degradation by functional metaproteomics (protein-SIP), Proteomics. (2013). doi:10.1002/pmic.201200569.

[9] M. Taubert, S. Baumann, M. Von Bergen, J. Seifert, Exploring the limits of robust detection of incorporation of 13C by mass spectrometry in protein-based stable isotope probing (protein-SIP), Anal. Bioanal. Chem. (2011). doi:10.1007/s00216-011-5289-4.

[10] M. Taubert, C. Vogt, T. Wubet, S. Kleinsteuber, M.T. Tarkka, H. Harms, F. Buscot, H.H. Richnow, M. Von Bergen, J. Seifert, Protein-SIP enables time-resolved analysis of the carbon flux in a sulfate-reducing, benzene-degrading microbial consortium, ISME J. (2012). doi:10.1038/ismej.2012.68.

[11] M. Taubert, N. Jehmlich, C. Vogt, H.H. Richnow, F. Schmidt, M. von Bergen, J. Seifert, Time resolved protein-based stable isotope probing (Protein-SIP) analysis allows quantification of induced proteins in substrate shift experiments, Proteomics. (2011). doi:10.1002/pmic.201000788.

[12] R. Starke, A. Keller, N. Jehmlich, C. Vogt, H.H. Richnow, S. Kleinsteuber, M. von Bergen, J.

Seifert, Pulsed13C2-Acetate Protein-SIP Unveils Epsilonproteobacteria as Dominant Acetate Utilizers in a Sulfate-Reducing Microbial Community Mineralizing Benzene, Microb. Ecol. (2016). doi:10.1007/s00248-016-0731-y.

[13] R. Starke, R. Kermer, L. Ullmann-Zeunert, I.T. Baldwin, J. Seifert, F. Bastida, M. von Bergen, N. Jehmlich, Bacteria dominate the short-term assimilation of plant-derived N in soil, Soil Biol. Biochem. (2016). doi:10.1016/j.soilbio.2016.01.009.

[14] N.B. Justice, Z. Li, Y. Wang, S.E. Spaudling, A.C. Mosier, R.L. Hettich, C. Pan, J.F. Banfield, 15N- and 2H proteomic stable isotope probing links nitrogen flow to archaeal heterotrophic activity, Environ. Microbiol. (2014). doi:10.1111/1462-2920.12488.

[15] J. Seifert, M. Taubert, N. Jehmlich, F. Schmidt, U. Völker, C. Vogt, H.H. Richnow, M. Von Bergen, Protein-based stable isotope probing (protein-SIP) in functional metaproteomics, Mass Spectrom. Rev. (2012). doi:10.1002/mas.21346.

[16] N. Jehmlich, C. Vogt, V. Lünsmann, H.H. Richnow, M. von Bergen, Protein-SIP in environmental studies, Curr. Opin. Biotechnol. (2016). doi:10.1016/j.copbio.2016.04.010.

[17] S.J. Blazewicz, E. Schwartz, Dynamics of18O Incorporation from H218O into Soil Microbial DNA, Microb. Ecol. (2011). doi:10.1007/s00248-011-9826-7.

[18] E. Schwartz, Analyzing microorganisms in environmental samples using stable isotope probing with H218O, Cold Spring Harb. Protoc. (2009). doi:10.1101/pdb.prot5341.

[19] E. Schwartz, Characterization of growing microorganisms in soil by stable isotope probing with H218O, Appl. Environ. Microbiol. (2007). doi:10.1128/AEM.02021-06.

[20] R. Angel, R. Conrad, Elucidating the microbial resuscitation cascade in biological soil crusts following a simulated rain event, Environ. Microbiol. (2013). doi:10.1111/1462-2920.12140.

[21] E.A. Rettedal, V.S. Brözel, Characterizing the diversity of active bacteria in soil by comprehensive stable isotope probing of DNA and RNA with H218O, Microbiologyopen. (2015). doi:10.1002/mbo3.230.

[22] M. Taubert, S. Stöckel, P. Geesink, S. Girnus, N. Jehmlich, M. von Bergen, P. Rösch, J. Popp, K. Küsel, Tracking active groundwater microbes with D2O labelling to understand their ecosystem function, Environ. Microbiol. (2018). doi:10.1111/1462-2920.14010.

[23] W. Bild, V. Nastasa, I. Haulica, In vivo and in vitro research on the biological effects of deuterium-depleted water: 1. Influence of deuterium-depleted water on cultured cell growth, Rom. J. Physiol. Physiol. Sci. (2004) 53–67.

[24] J.J. Katz, The Biology of Heavy Water, Sci. Am. 203 (1960) 106–117.

[25] O. V. Mosin, I. Ignatov, D.A. Skladnev, V.I. Shvets, Studying of Phenomenon of Biological Adaptation to Heavy Water, Russ. Fed. Eur. J. Mol. Biotechnol. 6 (2013) 180–209.

[26] C. Opitz, E. Ahrné, K.N. Goldie, A. Schmidt, S. Grzesiek, Deuterium induces a distinctive Escherichia coli proteome that correlates with the reduction in growth rate, J. Biol. Chem. (2019). doi:10.1074/jbc.RA118.006914.

[27] T. Sachsenberg, F.A. Herbst, M. Taubert, R. Kermer, N. Jehmlich, M. Von Bergen, J. Seifert, O. Kohlbacher, MetaProSIP: Automated inference of stable isotope incorporation

rates in proteins for functional metaproteomics, J. Proteome Res. (2015). doi:10.1021/pr500245w.

[28] R. Busch, Y.K. Kim, R.A. Neese, V. Schade-Serin, M. Collins, M. Awada, J.L. Gardner, C. Beysen, M.E. Marino, L.M. Misell, M.K. Hellerstein, Measurement of protein turnover rates by heavy water labeling of nonessential amino acids, Biochim. Biophys. Acta - Gen. Subj. (2006). doi:10.1016/j.bbagen.2005.12.023.

[29] L.A. Carpino, G.Y. Han, The 9-Fluorenylmethoxycarbonyl Amino-Protecting Group, J. Org. Chem. (1979). doi:10.1021/jo01335a600.

[30] I.I. Stewart, T. Thomson, D. Figeys, O labeling: A tool for proteomics, Rapid Commun. Mass Spectrom. (2001). doi:10.1002/rcm.525.

[31] L. Polgár, The catalytic triad of serine peptidases, Cell. Mol. Life Sci. (2005). doi:10.1007/s00018-005-5160-x.

[32] S.H. Duncan, A. Belenguer, G. Holtrop, A.M. Johnstone, H.J. Flint, G.E. Lobley, Reduced dietary intake of carbohydrates by obese subjects results in decreased concentrations of butyrate and butyrate-producing bacteria in feces, Appl. Environ. Microbiol. (2007). doi:10.1128/AEM.02340-06.

[33] W.R. Russell, S.W. Gratz, S.H. Duncan, G. Holtrop, J. Ince, L. Scobbie, G. Duncan, A.M. Johnstone, G.E. Lobley, R.J. Wallace, G.G. Duthie, H.J. Flint, High-protein, reduced-carbohydrate weight-loss diets promote metabolite profiles likely to be detrimental to colonic health, Am. J. Clin. Nutr. (2011). doi:10.3945/ajcn.110.002188.

[34] S.W. Englander, N.R. Kallenbach, Hydrogen exchange and structural dynamics of proteins and nucleic acids, Q. Rev. Biophys. (1983). doi:10.1017/S0033583500005217.

[35] S. Matysik, C.I. Le Roy, G. Liebisch, S.P. Claus, Metabolomics of fecal samples: A practical consideration, Trends Food Sci. Technol. (2016). doi:10.1016/j.tifs.2016.05.011.

[36] M.N. Price, G.M. Zane, J. V. Kuehl, R.A. Melnyk, J.D. Wall, A.M. Deutschbauer, A.P. Arkin, Filling gaps in bacterial amino acid biosynthesis pathways with high-throughput genetics, PLoS Genet. (2018). doi:10.1371/journal.pgen.1007147.

[37] X. Gao, E. Pujos-Guillot, J.F. Martin, P. Galan, C. Juste, W. Jia, J.L. Sebedio, Metabolite analysis of human fecal water by gas chromatography/mass spectrometry with ethyl chloroformate derivatization, Anal. Biochem. (2009). doi:10.1016/j.ab.2009.06.036.

[38] M. Neumann-Schaal, J.D. Hofmann, S.E. Will, D. Schomburg, Time-resolved amino acid uptake of Clostridium difficile 630Δerm and concomitant fermentation product and toxin formation, BMC Microbiol. (2015). doi:10.1186/s12866-015-0614-2.

[39] T.E. Rogers, N.A. Pudlo, N.M. Koropatkin, J.S.K. Bell, M. Moya Balasch, K. Jasker, E.C. Martens, Dynamic responses of Bacteroides thetaiotaomicron during growth on glycan mixtures, Mol. Microbiol. (2013). doi:10.1111/mmi.12228.

[40] C.H.F. Lau, D. Hughes, K. Poole, MexY-promoted aminoglycoside resistance in Pseudomonas aeruginosa: Involvement of a putative proximal binding pocket in aminoglycoside recognition, MBio. (2014). doi:10.1128/mBio.01068-14.

[41] M.S. Desai, A.M. Seekatz, N.M. Koropatkin, N. Kamada, C.A. Hickey, M. Wolter, N.A.

583 Pudlo, S. Kitamoto, N. Terrapon, A. Muller, V.B. Young, B. Henrissat, P. Wilmes, T.S.
584 Stappenbeck, G. Núñez, E.C. Martens, A Dietary Fiber-Deprived Gut Microbiota Degrades
585 the Colonic Mucus Barrier and Enhances Pathogen Susceptibility, Cell. (2016).
586 doi:10.1016/j.cell.2016.10.043.

587 [42] H.J. Flint, S.H. Duncan, K.P. Scott, P. Louis, Links between diet, gut microbiota
588 composition and gut metabolism, in: Proc. Nutr. Soc., 2015.
589 doi:10.1017/S0029665114001463.

590 [43] A.W. Walker, J. Ince, S.H. Duncan, L.M. Webster, G. Holtrop, X. Ze, D. Brown, M.D. Stares,
591 P. Scott, A. Bergerat, P. Louis, F. McIntosh, A.M. Johnstone, G.E. Lobley, J. Parkhill, H.J.
592 Flint, Dominant and diet-responsive groups of bacteria within the human colonic
593 microbiota, ISME J. (2011). doi:10.1038/ismej.2010.118.

594 [44] H.J. Flint, K.P. Scott, S.H. Duncan, P. Louis, E. Forano, Microbial degradation of complex
595 carbohydrates in the gut, Gut Microbes. (2012). doi:10.4161/gmic.19897.

596 [45] A. Rogowski, J.A. Briggs, J.C. Mortimer, T. Tryfona, N. Terrapon, E.C. Lowe, A. Baslé, C.
597 Morland, A.M. Day, H. Zheng, T.E. Rogers, P. Thompson, A.R. Hawkins, M.P. Yadav, B.
598 Henrissat, E.C. Martens, P. Dupree, H.J. Gilbert, D.N. Bolam, Glycan complexity dictates
599 microbial resource allocation in the large intestine, Nat. Commun. (2015).
600 doi:10.1038/ncomms8481.

601 [46] X. Ze, S.H. Duncan, P. Louis, H.J. Flint, Ruminococcus bromii is a keystone species for the
602 degradation of resistant starch in the human colon, ISME J. (2012).

603 doi:10.1038/ismej.2012.4.

604 [47] E.P. Halmos, C.T. Christophersen, A.R. Bird, S.J. Shepherd, P.R. Gibson, J.G. Muir, Diets
605 that differ in their FODMAP content alter the colonic luminal microenvironment, Gut.
606 (2015). doi:10.1136/gutjnl-2014-307264.

607 [48] A. Everard, V. Lazarevic, M. Derrien, M. Girard, G.M. Muccioli, A.M. Neyrinck, S.
608 Possemiers, A. Van Holle, P. François, W.M. De Vos, N.M. Delzenne, J. Schrenzel, P.D.
609 Cani, Responses of gut microbiota and glucose and lipid metabolism to prebiotics in
610 genetic obese and diet-induced leptin-resistant mice, Diabetes. (2011).
611 doi:10.2337/db11-0227.

612 [49] A. Everard, C. Belzer, L. Geurts, J.P. Ouwerkerk, C. Druart, L.B. Bindels, Y. Guiot, M.
613 Derrien, G.G. Muccioli, N.M. Delzenne, W.M. de Vos, P.D. Cani, Cross-talk between
614 Akkermansia muciniphila and intestinal epithelium controls diet-induced obesity, Proc.
615 Natl. Acad. Sci. (2013). doi:10.1073/pnas.1219451110.

616 [50] G.D. Wu, J. Chen, C. Hoffmann, K. Bittinger, Y.Y. Chen, S.A. Keilbaugh, M. Bewtra, D.
617 Knights, W.A. Walters, R. Knight, R. Sinha, E. Gilroy, K. Gupta, R. Baldassano, L. Nessel, H.
618 Li, F.D. Bushman, J.D. Lewis, Linking long-term dietary patterns with gut microbial
619 enterotypes, Science (80-.). (2011). doi:10.1126/science.1208344.

620 [51] L.A. David, C.F. Maurice, R.N. Carmody, D.B. Gootenberg, J.E. Button, B.E. Wolfe, A. V.
621 Ling, A.S. Devlin, Y. Varma, M.A. Fischbach, S.B. Biddinger, R.J. Dutton, P.J. Turnbaugh,
622 Diet rapidly and reproducibly alters the human gut microbiome, Nature. (2014).

623 doi:10.1038/nature12820.

624 [52] K.P. Geboes, G. De Hertogh, V. De Preter, A. Luypaerts, B. Bammens, P. Evenepoel, Y.
625 Ghoos, K. Geboes, P. Rutgeerts, K. Verbeke, The influence of inulin on the absorption of
626 nitrogen and the production of metabolites of protein fermentation in the colon, Br. J.
627 Nutr. (2006). doi:10.1017/BJN20061936.

628 [53] R. Starke, P. Capek, D. Morais, S.J. Callister, N. Jehmlich, The total microbiome functions
629 in bacteria and fungi, J. Proteomics. (2020). doi:10.1016/j.jprot.2019.103623.

630 [54] R. Starke, P. Capek, D. Morais, N. Jehmlich, P. Baldrian, Explorative Meta-Analysis of 377
631 Extant Fungal Genomes Predicted a Total Mycobiome Functionality of 42.4 Million KEGG
632 Functions, Front. Microbiol. 11 (2020) 143.

633 [55] S. Yen, J.A.K. McDonald, K. Schroeter, K. Oliphant, S. Sokolenko, E.J.M. Blondeel, E. Allen-
634 Vercoe, M.G. Aucoin, Metabolomic analysis of human fecal microbiota: A comparison of
635 feces-derived communities and defined mixed communities, J. Proteome Res. (2015).
636 doi:10.1021/pr5011247.

637 [56] M. Marzorati, R. Vilchez-Vargas, J. Vanden Bussche, P. Truchado, R. Jauregui, R.A. El
638 Hage, D.H. Pieper, L. Vanhaecke, T. Van de Wiele, High-fiber and high-protein diets shape
639 different gut microbial communities, which ecologically behave similarly under stress
640 conditions, as shown in a gastrointestinal simulator, Mol. Nutr. Food Res. (2017).
641 doi:10.1002/mnfr.201600150.

642 [57] J.A.K. McDonald, S. Fuentes, K. Schroeter, I. Heikamp-deJong, C.M. Khursigara, W.M. de

643 Vos, E. Allen-Vercoe, Simulating distal gut mucosal and luminal communities using
644 packed-column biofilm reactors and an in vitro chemostat model, J. Microbiol. Methods.
645 (2015). doi:10.1016/j.mimet.2014.11.007.

646 [58] U.K. Laemmli, Cleavage of structural proteins during the assembly of the head of
647 bacteriophage T4, Nature. (1970). doi:10.1038/227680a0.

648 [59] N. Jehmlich, F. Schmidt, M. Hartwich, M. Von Bergen, H.H. Richnow, C. Vogt,
649 Incorporation of carbon and nitrogen atoms into proteins measured by protein-based
650 stable isotope probing (Protein-SIP), Rapid Commun. Mass Spectrom. (2008).
651 doi:10.1002/rcm.3684.

652 [60] H.L. Röst, T. Sachsenberg, S. Aiche, C. Bielow, H. Weisser, F. Aicheler, S. Andreotti, H.C.
653 Ehrlich, P. Gutenbrunner, E. Kenar, X. Liang, S. Nahnsen, L. Nilse, J. Pfeuffer, G.
654 Rosenberger, M. Rurik, U. Schmitt, J. Veit, M. Walzer, D. Wojnar, W.E. Wolski, O.
655 Schilling, J.S. Choudhary, L. Malmström, R. Aebersold, K. Reinert, O. Kohlbacher,
656 OpenMS: A flexible open-source software platform for mass spectrometry data analysis,
657 Nat. Methods. (2016). doi:10.1038/nmeth.3959.

658

659 **Figure legends**

660 **Figure 1. Validation of deuterium and ^{18}O incorporation.** The pipeline was validated by the
661 standards D5-Angiotensin II at different labeling ratios (c) and BSA tryptically digested in different
662 RIA of ^{18}O-water (e) and *E. coli* K12 grown in 25% and 50% D_2O (d) or $H_2{}^{18}O$ (f). An exemplary
663 incorporation pattern of D (a) and ^{18}O (b) into one peptide each produced by *E. coli* K12 is
664 depicted. The number of labeled peptides is indicated for each boxplot. Median, lower and upper
665 quartiles, lower and upper whiskers, 5th and 95th percentiles, and the detection limit are shown
666 in the boxplots (n=3).

667 **Figure 2. Workflow and global correlation of metabolic activity and isotope incorporation.** The
668 workflow of the labelling experiment (a) and the RIA of all measured peptides within the
669 microbial community (b) are shown for D (in red) and ^{18}O (in blue). The species-specific difference
670 between high fiber (HF) and high protein diet (HP) in RIA and LR are depicted for D (in red) and
671 ^{18}O (in blue) with the 20 most active organisms that contribute at least 90% of abundance within
672 16S rRNA DNA amplicons, metaproteome, and protein-SIP.

673 **Figure 3. Taxonomic correlation of metabolic activity and label incorporation.** The relative
674 abundances of the 20 most active species are shown as bubble sizes for relative area under the
675 curve (metaproteome), relative counts of labeled peptides (SIP RA) and relative isotope
676 abundance (SIP RIA) in regards to medium (P – high protein, F – high fiber) and treatment (0 –
677 inoculum, Ctrl – unlabeled water, D – D_2O, 18O – $H_2{}^{18}O$).

678 **Figure 4. Functional correlation of metabolic activity and label incorporation.** A volcano-plot
679 depicting the log2 fold change between high fiber (as positive values) and high protein diet (as

680 negative values), and the corresponding p-values. The different shades represent different COG

681 classes.

682 **Figure 5. Incorporation routes for ^{18}O into amino acids.** The stable and unstable (if cleaved or at

683 carboxylic groups) incorporation routes into amino acids as a precursor of proteins are depicted.

684

Data availability

Supplementary information is provided.

Acknowledgments

The authors acknowledge the National Sciences and Engineering Research Council of Canada scholarship and Ontario Ministry of Advanced Education and Skills Development scholarship to KO for providing funding. MvB and SS acknowledge funding by DFG Priority program SPP 1656 “Microbiota and Inflammation”. RS acknowledges funding by CRC Aquadiva and thanks to the Czech Science Foundation for the project 20-02022Y. OK and TS acknowledge funding from the German Ministry of Research and Education (BMBF, grant 031A535A).

Table 1

Diet	Pathway	Enrichment FDR	Translated genes	Total genes
High fiber	KEGG	7.28E-97	104	656
High fiber	KEGG	9.65E-51	53	277
High fiber	KEGG	2.19E-28	27	111
High fiber	KEGG	8.40E-24	31	241
High fiber	KEGG	6.02E-17	12	25
High fiber	KEGG	1.99E-16	17	86
High fiber	KEGG	1.99E-14	12	38
High fiber	KEGG	7.43E-14	16	103
High fiber	KEGG	1.25E-12	10	29
High fiber	KEGG	6.54E-11	11	56
High protein	KEGG	1.35E-57	32	56
High protein	KEGG	1.43E-45	52	656
High protein	KEGG	9.61E-28	29	277
High protein	KEGG	6.15E-23	19	103
High protein	KEGG	9.47E-20	22	241
High protein	KEGG	2.07E-10	11	111
High protein	KEGG	2.25E-10	8	40
High protein	KEGG	2.25E-10	10	86
High protein	KEGG	2.25E-10	8	39
High protein	KEGG	6.15E-09	7	38
High fiber	ECOCYC	4.02E-26	21	55
High fiber	ECOCYC	8.75E-15	12	32
High fiber	ECOCYC	7.68E-10	7	14
High fiber	ECOCYC	7.68E-10	6	8
High fiber	ECOCYC	1.65E-08	6	12
High fiber	ECOCYC	2.53E-08	6	13
High fiber	ECOCYC	1.22E-06	4	6
High fiber	ECOCYC	1.22E-06	4	6
High fiber	ECOCYC	1.22E-06	5	13
High fiber	ECOCYC	1.22E-06	5	13
High protein	ECOCYC	8.74E-17	13	55
High protein	ECOCYC	1.60E-14	10	32
High protein	ECOCYC	4.21E-12	7	14
High protein	ECOCYC	3.12E-09	6	18
High protein	ECOCYC	4.31E-09	6	20
High protein	ECOCYC	4.31E-09	4	4
High protein	ECOCYC	5.15E-09	6	21
High protein	ECOCYC	6.16E-09	6	22
High protein	ECOCYC	1.28E-08	6	25
High protein	ECOCYC	2.53E-08	5	14

Functional Category
Metabolic pathways
Biosynthesis of secondary metabolites
Biosynthesis of amino acids
Microbial metabolism in diverse environments
Aminoacyl-tRNA biosynthesis
Purine metabolism
Arginine and proline metabolism
Carbon metabolism
Alanine; aspartate and glutamate metabolism
Ribosome
Ribosome
Metabolic pathways
Biosynthesis of secondary metabolites
Carbon metabolism
Microbial metabolism in diverse environments
Biosynthesis of amino acids
Glycolysis / Gluconeogenesis
Purine metabolism
Amino sugar and nucleotide sugar metabolism
Fructose and mannose metabolism
superpathway of histidine; purine; and pyrimidine biosynthesis
purine nucleotides de novo biosynthesis I
adenosine nucleotides de novo biosynthesis
starch degradation V
arginine biosynthesis II (acetyl cycle)
arginine biosynthesis I
5-aminoimidazole ribonucleotide biosynthesis II
superpathway of 5-aminoimidazole ribonucleotide biosynthesis
purine nucleotides de novo biosynthesis II
superpathway of pyrimidine ribonucleotides de novo biosynthesis
superpathway of histidine; purine; and pyrimidine biosynthesis
purine nucleotides de novo biosynthesis I
adenosine nucleotides de novo biosynthesis
glycolysis III (glucokinase)
glycolysis I
GDP-mannose biosynthesis
gluconeogenesis I
superpathway of glycolysis; pyruvate dehydrogenase; TCA; and glyoxylate bypass
superpathway of glycolysis and Entner-Doudoroff
TCA cycle VI (obligate autotrophs)

Figure 1

Click here to access/download;Figure;Figure 1.tif

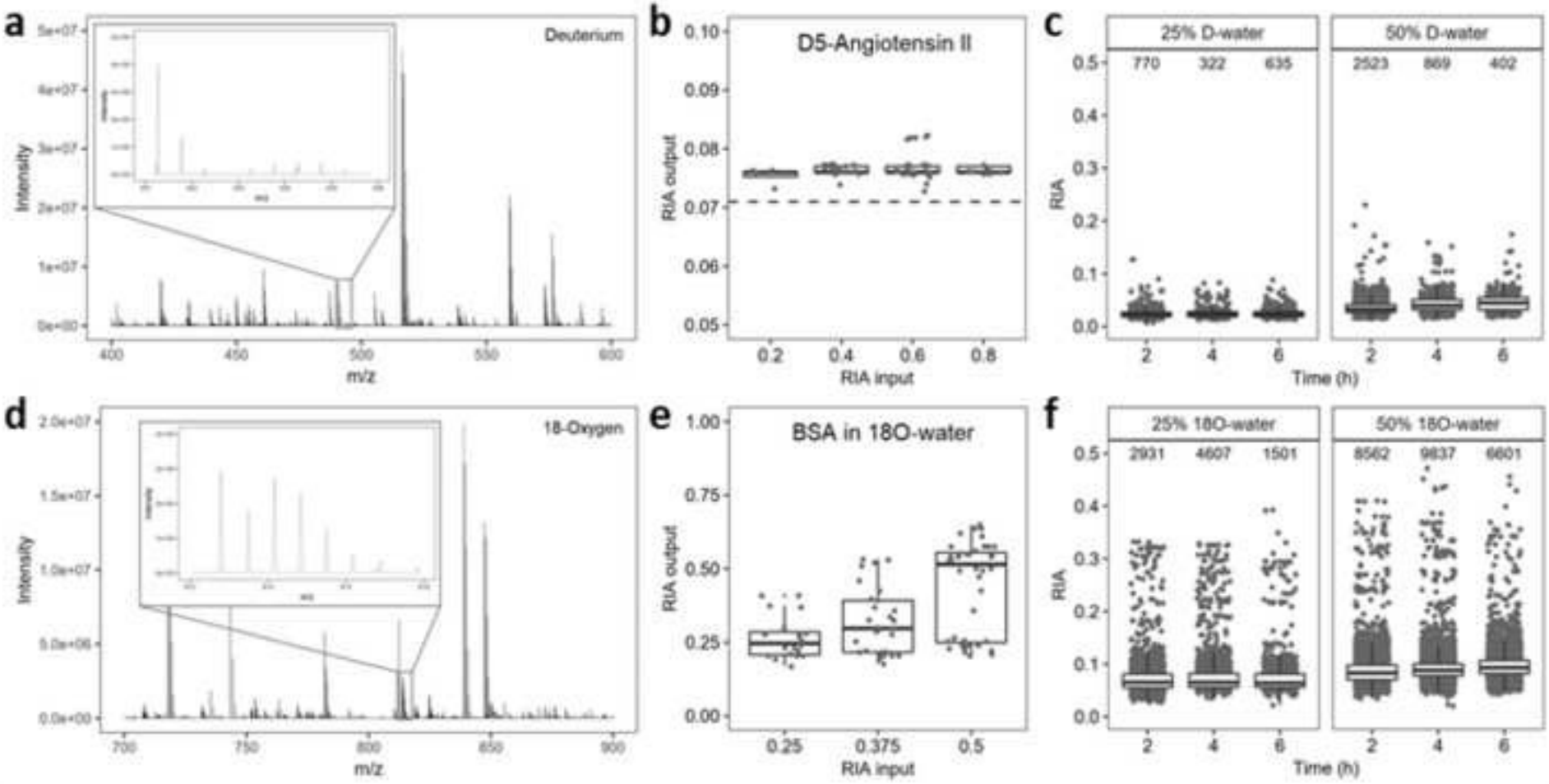

Figure 2

Click here to access/download;Figure;Figure 2.tif

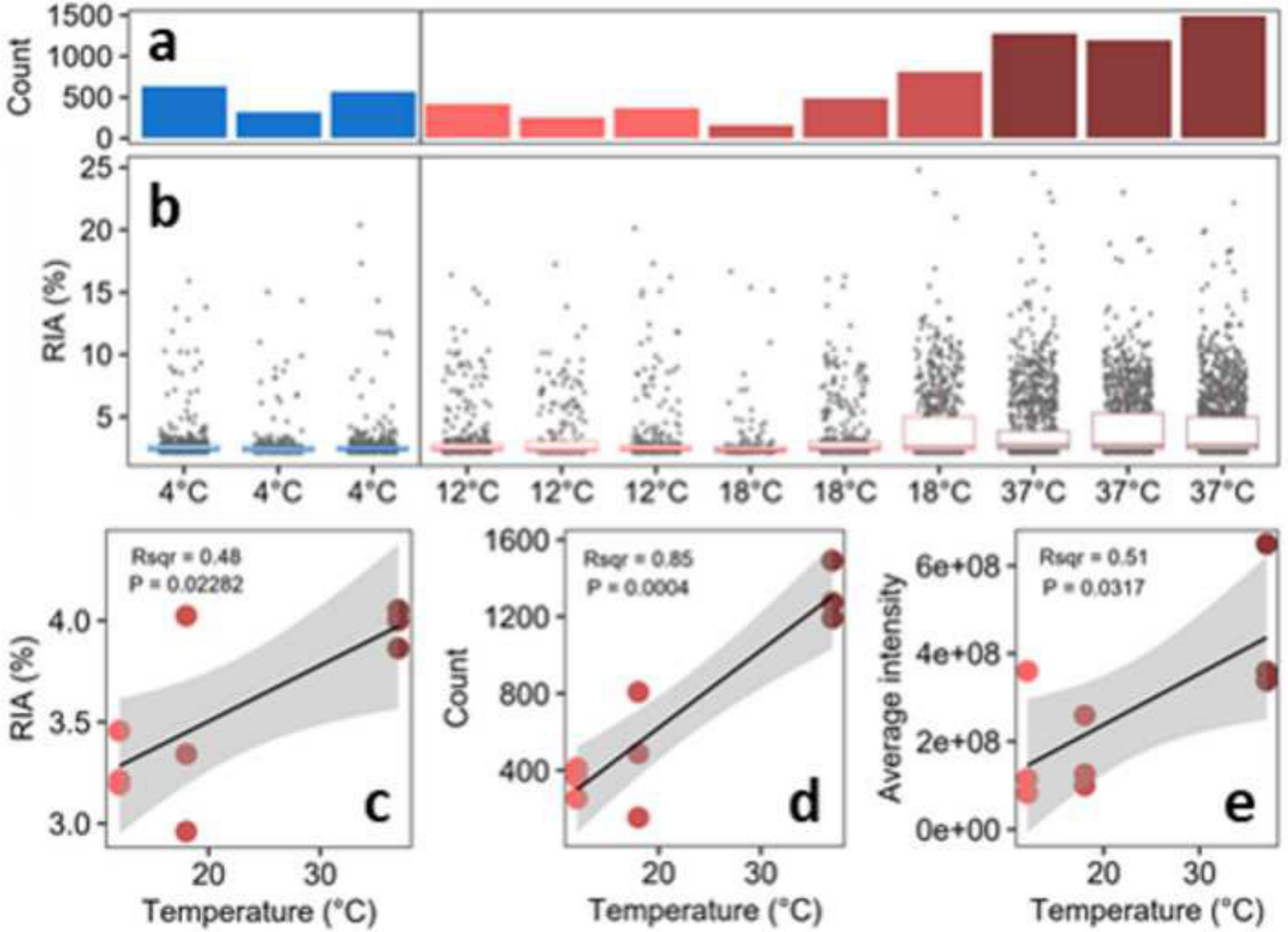

Figure 3

Click here to access/download;Figure;Figure 3 - neu.tif

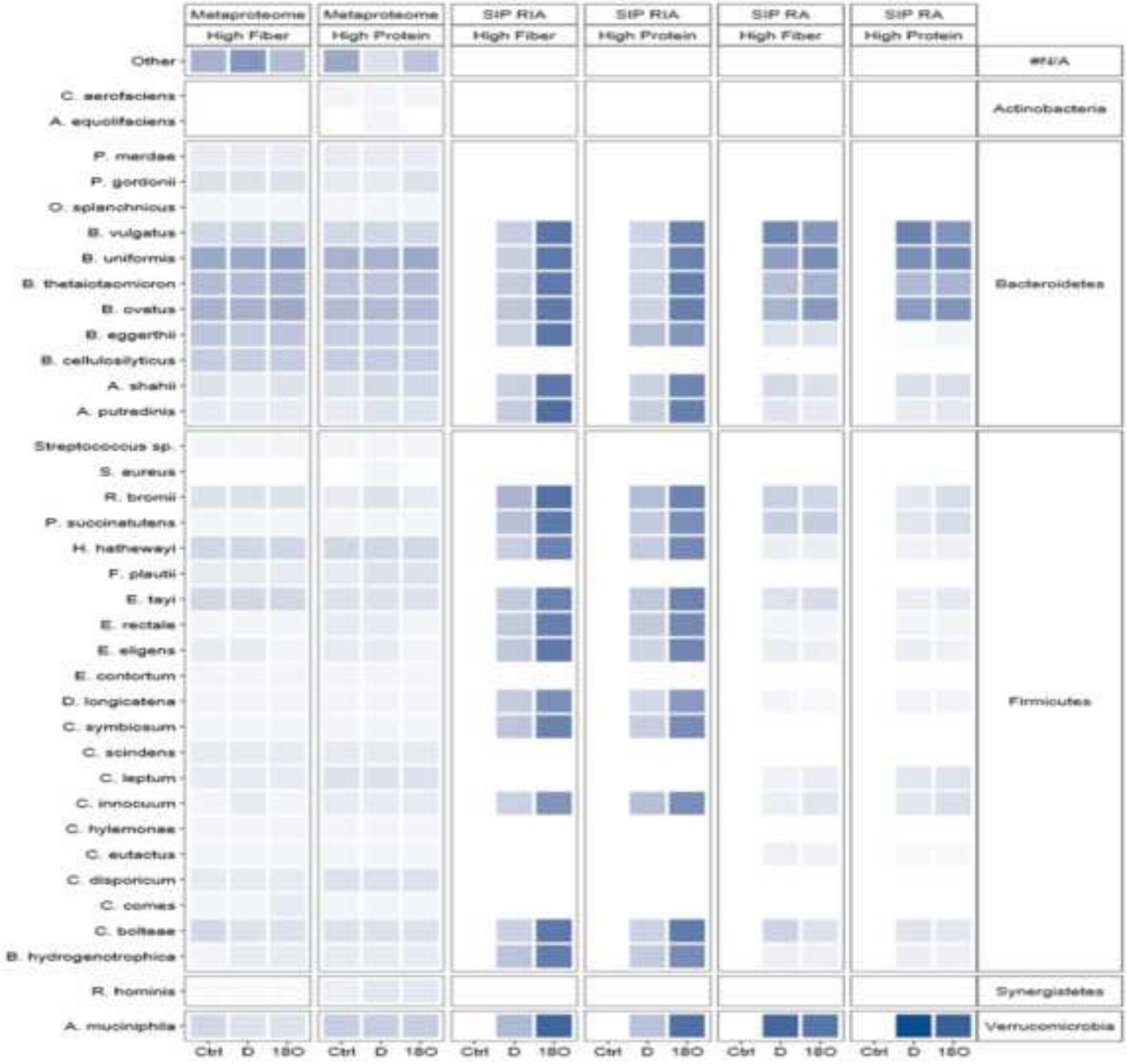

Figure 4

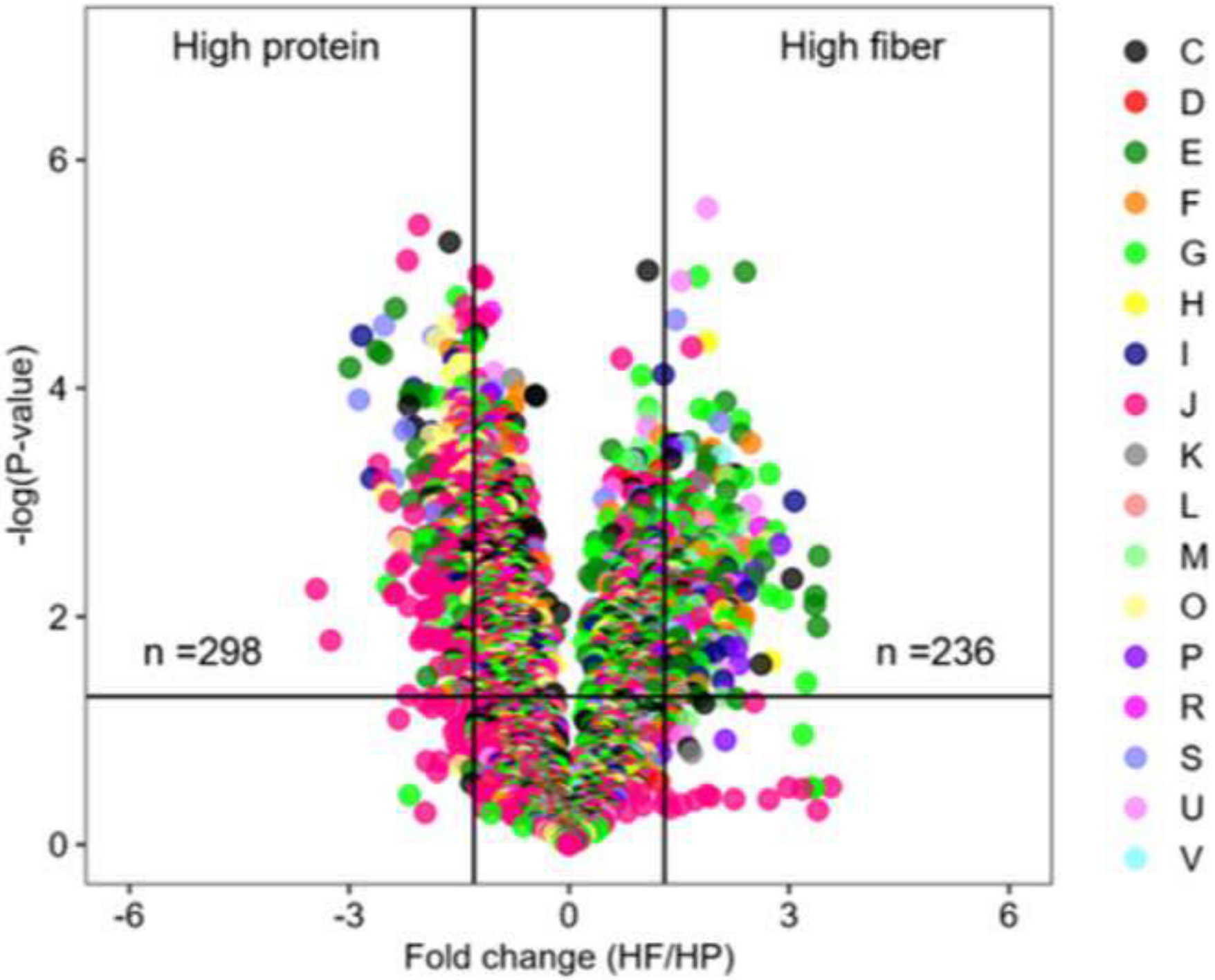

Figure 5